Relevance of silicon isotopes to Si-nutrient utilization and Si-source assessment in Antarctic waters

D. Cardinal,[1] L. Y. Alleman,[1,2] F. Dehairs,[3] N. Savoye,[3] T. W. Trull,[4] and L. André[1]

Received 25 August 2004; revised 6 December 2004; accepted 15 February 2005; published 15 April 2005.

[1] We analyzed δ^{29}Si of dissolved silicate for eight water column profiles across the Southern Ocean (south of Australia in spring 2001) from the Seasonal Ice Zone (SIZ) north to the Subantarctic Zone (SAZ), including the first isotopic compositions measured for Si-depleted seawaters. All profiles display mixed layer enrichments in heavy Si isotopes relative to deep water in accordance with preferential uptake of the light isotope by diatoms. As silicate levels decrease from the SIZ northward across the Polar Front Zone (PFZ) to the SAZ, surface and mesopelagic δ^{29}Si signatures generally become progressively heavier, but the most Si-depleted SAZ waters do not exhibit δ^{29}Si values heavier than in the PFZ. This intricacy appears to derive from variations in the vertical and horizontal supply of silicate to surface waters, and by applying a steady state open system model, we estimate a fractionation factor, $^{29}\varepsilon$, between diatoms and seawater of -0.45 ± 0.17‰, independently of zones and phytoplankton community. Though encouraging, these results are related to latitudinal changes in mesopelagic δ^{29}Si values, complexity in surface silicate$-\delta^{29}$Si correlations, and differences from previous studies, which underline the need for caution in the use of silicon isotopes in paleoceanographic studies until systematic efforts have been undertaken to better understand modern variations.

Citation: Cardinal, D., L. Y. Alleman, F. Dehairs, N. Savoye, T. W. Trull, and L. André (2005), Relevance of silicon isotopes to Si-nutrient utilization and Si-source assessment in Antarctic waters, *Global Biogeochem. Cycles*, *19*, GB2007, doi:10.1029/2004GB002364.

1. Introduction

[2] The Southern Ocean is a major player in the global carbon cycle. Although it represents less than 10% of the open ocean, its High Nitrate–Low Chlorophyll (HNLC) waters account for more than 20% of the modern global ocean carbon sink [*Metzl et al.*, 1999; *Takahashi et al.*, 2002]. Its coupling with the global thermohaline oceanic circulation makes it a key factor for controlling oceanic biogeochemical cycles even at low latitudes [*Rintoul et al.*, 2001]. Southern Ocean waters supply nutrients to tropical and equatorial areas [*Brzezinski et al.*, 2002] and even into the North Atlantic Ocean [*Sarmiento et al.*, 2004]. This nutrient supply could account for three quarters of the export production north of 30°S. Greater depletion of silicate (or silicic acid, $Si(OH)_4$), by diatoms in the Southern Ocean relative to nitrate and phosphate [*Dugdale et al.*, 1995; *Trull et al.*, 2001a; *Nelson et al.*, 2001; *Brzezinski et al.*, 2002; *Coale et al.*, 2004], separates the supply pathways of Si, N, and P to the rest of the ocean, and restricts diatoms to the role of a relatively minor phytoplankton group in most of the other oceanic provinces [*Yool and Tyrrell*, 2003]. The hypothesis of a larger silicic acid leakage to northern latitudes has recently been explored in order to explain the low glacial atmospheric CO_2 levels [*Matsumoto et al.*, 2002]. Similarly, paleovariations of silicate availability and utilization in response to stratification changes and a larger supply of the Fe micronutrient have been considered to be important in increasing glacial Southern Ocean productivity and contributing to lower glacial atmospheric CO_2 levels [*Martin*, 1990; *François et al.*, 1997; *Popova et al.*, 2000; *Watson et al.*, 2000].

[3] To address these and other aspects of global marine biogeochemical cycles and global change modeling, the assessment of nutrient utilization efficiency and co-limitation by phytoplankton is essential. Silicon isotope variations are important to this effort because they offer a means to track the sources and magnitudes of silicon transports and transformations within the ocean. The silicon isotopic compositions of diatoms have been used for this purpose, in particular as a paleoproxy of silicic acid utilization in the Southern Ocean [*De La Rocha et al.*, 1998; *Brzezinski et al.*, 2002]. Indeed the silicon isotope fractionation factor between seawater and diatoms has been found to be independent of temperature

[1]Department of Geology and Mineralogy, Musée Royal de l'Afrique Centrale, Tervuren, Belgium.
[2]Now at Ecole Supérieure des Mines de Douai, Douai, France.
[3]Department of Analytical and Environmental Chemistry, Vrije Universiteit Brussel, Brussels, Belgium.
[4]Antarctic Climate and Ecosystem Cooperative Research Centre, CSIRO Marine Research, University of Tasmania, Hobart, Tasmania, Australia.

0886-6236/05/2004GB002364

(12°–22°C) and species [*De La Rocha et al.*, 1997]. Recent studies on physiological aspects [*Milligan et al.*, 2004] and freshwater ecosystems [*Alleman et al.*, 2004] have confirmed the broad applicability of this proxy and its great potential in paleoceanography [*Henderson*, 2002]. *Wischmeyer et al.* [2003] calculated the silicon isotope behavior of dissolved and diatom fractions in the world ocean using current understanding of Si isotope cycle (e.g., diatom - seawater fractionation factor [*De La Rocha et al.*, 1997]) in an Ocean General Circulation Model (HAMMOC4). They discussed the modeled seasonal and spatial variations of Si isotopic signature in regard to fractionation processes. Until now the only data to test and support this modeling study of the silicon isotopes cycle and its associated assumptions were those reported by *De La Rocha et al.* [2000] and *Varela et al.* [2004]. Notably, there have been no observations of the isotopic composition for Si-depleted surface waters and no measurements of complete water column profiles in the open ocean. To fill this gap and better constrain silicon isotopes as a proxy of silicic acid utilization, this study presents the first series of complete water column profiles of dissolved silicon isotopic compositions from the subantarctic to the sea ice zones in the spring Southern Ocean, south of Australia. This work also provides the first isotopic compositions of silicic acid depleted subantarctic surface waters (2–10 μmol L^{-1}). We discuss a spatially well-resolved isotopic data set (eight stations combining more than 90 isotopic compositions in total) along the WOCE-SR3 line in terms of latitudinal variations, diatom abundance, Si-nutrient sources and utilization, proxy validation, and oceanic circulation.

2. Material and Methods

[4] Sampling occurred during late spring 2001 along a north-south transect at 140°E–144°E (CLIVAR SR3, cruise AU0103, 29 October to 11 December 2001, R/V *Aurora Australis*), in the Australian sector (Figure 1). The eight sampling stations were located in the following Antarctic zones (defined and described by *Orsi et al.* [1995]; *Trull et al.* [2001a], and *Rintoul et al.* [2001]): the Subantarctic Zone (SAZ: 46.9°S and 48.8°S); the Subantarctic Front (SAF: 51.0°S); the Polar Front Zone (PFZ: 53.7°S); the Interpolar Frontal Zone (IPFZ: 56.9°S); the southern Antarctic Zone (AZ-S: 60.8°S) as well as two stations under sea ice influence located between the Southern Antarctic Circumpolar Front (SACCF) and the Southern Boundary (63.9°S) and between the SB and the Antarctic Slope Front (64.9°S). These two southernmost stations are reported below as located in the Seasonal Ice Zone (SIZ). The station at 63.9°S was the only one covered by sea ice at the time of sampling, while for the station at 64.9°S, visited 10 days later, melting had taken place and sampling occurred in partially ice-free conditions.

[5] Seawater was collected using CTD Rosette Niskin bottles. Water samples were immediately filtered through 0.4-μm polycarbonate membranes and stored at room temperature in the dark, in acid-cleaned polypropylene bottles. Samples were processed after return to the laboratory (MRAC, Tervuren). Silicon was precipitated following the

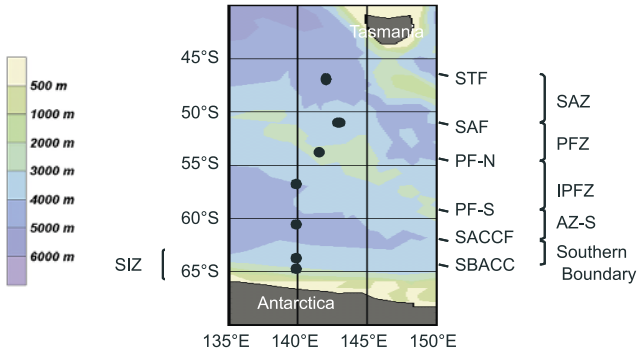

Figure 1. Sampling area. STF: Sub-Tropical Front; SAF: Sub-Antarctic Front; PF-N and PF-S: northern and southern branches of the Polar Front, respectively; SACCF, Southern Antarctic Circumpolar Current Front; SBACC, Southern Boundary of the Antarctic Circumpolar Current; SAZ, Sub-Antarctic Zone; PFZ, Polar Front Zone; IPFZ, Inter-Polar Front Zone; AZ-S, southern Antarctic Zone; SIZ, seasonal Ice Zone. See text and *Orsi et al.* [1995], *Trull et al.* [2001a], and *Rintoul et al.* [2001] for more details.

triethylamine molybdate co-precipitation method [*De La Rocha et al.*, 1996] (adapted from *de Freitas et al.* [1991]). Complete Si recovery was monitored by checking periodically that no detectable amount of silicic acid remained in the water after filtering the molybdate precipitate. After combustion of the silicomolybdate precipitate in covered Pt crucibles, the pure cristobalite phase was transferred to pre-cleaned polypropylene vials. Dissolution and isotopic measurements were then performed following the methodology described by *Cardinal et al.* [2003] for which the accuracy has been checked by intercalibration [*Cardinal et al.*, 2003; *Carignan et al.*, 2004]. Briefly, once the formed cristobalite was dissolved in a dilute HF/HCl mixture, Si isotopic analyses were carried out on a Nu Plasma MC-ICP-MS (ULB-MRAC, Brussels) using Mg external doping in dry plasma mode. To avoid matrix effects, systematic analyses of major elements (such as Mg, Ca, Na, K) were performed by ICP-AES in order to ensure the sample purity prior to isotopic analyses. As the Nu Plasma MC-ICP-MS does not resolve the isobaric interference of $^{14}N^{16}O$ on the ^{30}Si peak, results are calculated in ‰ relatively to the NBS28 quartz standard as $\delta^{29}Si$ [$\delta^{29}Si = [(^{29}Si/^{28}Si)_{sample}/(^{29}Si/^{28}Si)_{NBS28} - 1] \times 1000$]. Assuming a mass dependent fractionation, $\delta^{29}Si$ results can be converted into $\delta^{30}Si$ values by applying a multiplying factor of 1.93 [*De La Rocha*, 2002]. However, because conversion and comparison of isotopic compositions obtained originally from different isotope ratios is not straightforward [*Wombacher and Rehkämper*, 2004], we prefer to report and discuss our results using the actual $\delta^{29}Si$ notation [*Carignan et al.*, 2004]. Average analytical standard error was 0.030‰ (1σ) on $\delta^{29}Si$ (Table 1). Overall reproducibility of co-precipitation and isotopic analyses, assessed on 10 aliquots from the same seawater sample entirely processed individually, was ±0.07‰ (±2 σ) on $\delta^{29}Si$ (Table 1).

Table 1. Molybdate Coprecipitations' and $\delta^{29}Si$ Analyses' Replication[a]

Date of Run	ID Number	Volume Seawater, mL	$\delta^{29}Si$, ‰ Versus NBS28	Standard Error,[b] ‰
19 Feb. 2004	1	50	0.723	0.030
19 Feb. 2004	2	50	0.722	0.032
19 Feb. 2004	3	50	0.692	0.032
19 Feb. 2004	4	50	0.688	0.029
24 Feb. 2004	5	50	0.623	0.031
19 Feb. 2004	6	100	0.666	0.034
19 Feb. 2004	7	100	0.629	0.029
19 Feb. 2004	8	100	0.667	0.031
19 Feb. 2004	9	100	0.712	0.030
24 Feb. 2004	10	100	0.683	0.027
Average			0.681	0.030
Standard deviation			0.035	

[a]Ten aliquots (50 or 100 mL) were split from CTD124, 800m depth with a $Si(OH)_4$ content of 107.9 μmol L^{-1}. They were independently processed following *De La Rocha et al.* [1996] for precipitation and purification of $Si(OH)_4$ and then *Cardinal et al.* [2003] for the isotopic analyses.

[b]Standard error is the cumulated analytical error on Mg and Si isotopic ratios measured both on the standard and sample propagated to $\delta^{29}Si$ [see *Cardinal et al.*, 2003].

[6] For silicic acid concentrations ($[Si(OH)_4]$) less than ~10 μmol L^{-1}, the precipitation protocol is inefficient, so we applied an additional pre-concentration step adapted by *Brzezinski et al.* [2003a] from the MAGIC method [*Karl and Tien*, 1992]. It consists of precipitating $Si(OH)_4$ along with brucite ($Mg(OH)_2$) by increasing the pH with ammonium hydroxide, centrifugation, and redissolution in HCl. *Brzezinski et al.* [2003a] report that this method does not fractionate Si isotopes at the precision level usually required for isotopic dilution experiments. Since for natural isotopic signature studies the analytical precision must be at least an order of magnitude better, we verified that the MAGIC pre-concentration step as applied here did not induce any fractionation affecting the final $\delta^{29}Si$ results. Table 2 shows the $\delta^{29}Si$ for 6 CLIVAR-SR3 samples (10–16 μmol L^{-1} Si), analyzed with and without the pre-concentration step. The average $\delta^{29}Si$ difference between the two methods ($\Delta^{29}Si$) was +0.005‰, showing that there was no systematic isotopic bias toward heavier or lighter $\delta^{29}Si$. The absolute difference between samples and their replicates using pre-concentration is 0.07‰. These reproducibility results are similar to those observed for samples without pre-concentration (see Table 1). We have also checked for six seawater CLIVAR-SR3 samples (including four with silicate concentrations below 10 μmol L^{-1}) that there was complete recovery of Si after NH_4OH addition: No detectable amount of $Si(OH)_4$ was measured on the supernatant by acid-molybdate colorimetric method [*Strickland and Parsons*, 1968]. Since the minimum detectable value of the instrument was 0.2 μmol L^{-1}, this indicates a yield of recovery of at least 95%. Moreover, Si contents measured by ICP-AES in the brucite phase redissolved in HCl (i.e., before the TEA-Mo coprecipitation) also provide evidence of total recovery on these samples (99 ± 8%) relative to the initial $Si(OH)_4$ content. This complete recovery is an essential aspect of the successful application of the pre-concentration method.

3. Results

[7] Complete $\delta^{29}Si$ water column profiles are presented in Figure 2 and Table 3 along with the silicic acid profiles. All profiles display a heavier isotopic composition in surface relative to deep waters, similar to that commonly observed in the ocean for $\delta^{15}NO_3^-$ [*Sigman et al.*, 1999; *Altabet and François*, 2001; *Karsh et al.*, 2003]. Average $\delta^{29}Si$ signatures for different depth ranges were as follows: within the mixed layer, 0.97 ± 0.09‰ (n = 14); mesopelagic waters (200–1000 m), 0.70 ± 0.11‰ (n = 28); deep waters (>1800 m), 0.62 ± 0.06‰ (n = 30). These values are in good agreement with the few previous results from the Southern Ocean: 1.19 ± 0.25‰ (n = 8), 0.67 ± 0.05‰ (n = 5), 0.57 ± 0.04‰ (n = 9) for surface (spring samples from *Varela et al.* [2004]), intermediate, and deep [*De La Rocha et al.*, 2000] waters respectively. Our averaged deep-water signature is also close to the estimate of the oceanic steady state signature (0.70‰) in the model simulation study of *Wischmeyer et al.* [2003].

[8] $\delta^{29}Si$ and $[Si(OH)_4]$ profiles at 46.9 and 48.8°S in the SAZ superpose closely (Figure 2), except at 2000 m. This

Table 2. Replicates of $\delta^{29}Si$ Using Preconcentration Step[a]

			No Preconcentration		With Preconcentration			
CTD	Depth, m	$[Si(OH)_4]$, μmol L^{-1}	Run Number	$\delta^{29}Si$, ‰	Run Number	Volume, mL	$\delta^{29}Si$,[b] ‰	$\Delta^{29}Si$, ‰
17	300	3.8		NA	12672[c]	500	0.842 ± 37	
24	300	3.6		NA	12666[c]	500	0.933 ± 43	
24	500	4.1		NA	12670[c]	500	0.834 ± 35	
37	50	5		NA	12674[c]	335	1.127 ± 42	
37	300	10.4	6579	0.897 ± 37	12678[c]	250	1.024 ± 39	0.126
51	140	13.1	6212	1.073 ± 37	12668[c]	205	1.067 ± 39	−0.006
51	5	10.9	6203	1.023 ± 33	12445[d]	250	0.913 ± 42	−0.110
51	100	11.8	6210	0.972 ± 33	7672	250	0.992 ± 35	0.020
63	50	15.8	7625	0.965 ± 34	12538	500	0.885 ± 43	−0.080
63	100	16.2	8085	1.003 ± 38	12540	307	1.079 ± 43	0.076
All $\Delta^{29}Si$ average								0.005
Average of absolute $\Delta^{29}Si$								0.070

[a]NA denotes not applicable.

[b]Numbers after $\delta^{29}Si$ represent the analytical standard error of each isotopic signature (last two digits of the $\delta^{29}Si$).

[c]Total recovery of Si has been checked for these samples (see text for details).

[d]This sample has been diluted twice; that is, the actual Si content of the water before adding NH_4OH was 5.5 μmol Si L^{-1}.

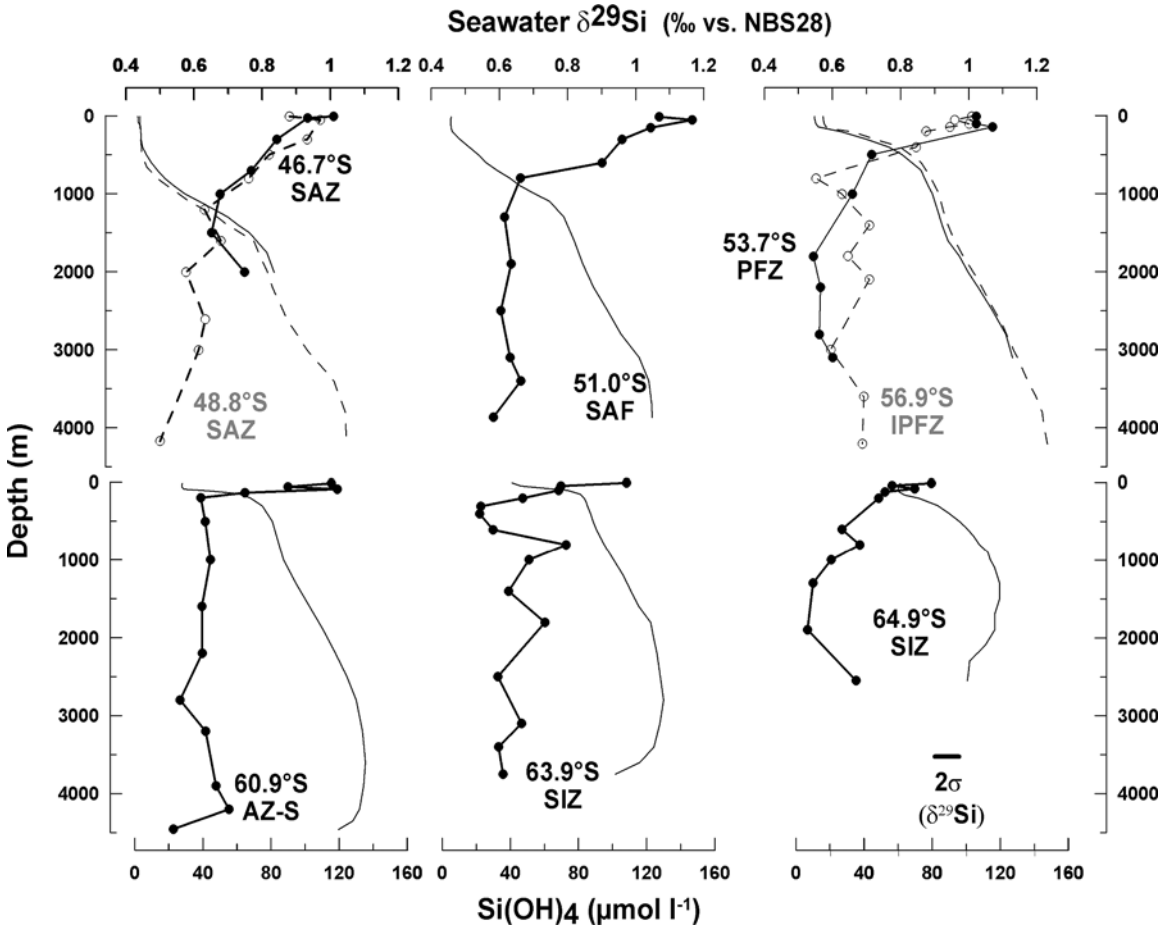

Figure 2. Seawater δ^{29}Si (circles) and $Si(OH)_4$ concentrations (lines without symbols) during CLIVAR-SR3. Average standard error (2 σ) of δ^{29}Si analyses is given (0.07‰). The stations were grouped in pairs whenever they are adjacent with comparable [$Si(OH)_4$] profiles. See caption of Figure 1 for details on zonal acronyms.

reflects the homogeneity of this zone in terms of prevalent water masses (see Figure 3) and of biogeochemical processes acting on the Si cycle. The upper 500 m of the SAZ consist of Subantarctic Mode Water (SAMW), a layer homogeneous in density and temperature [*Rintoul et al.*, 2001; *Sarmiento et al.*, 2004]. Surface waters at 51°S have δ^{29}Si values which differ from those in the SAZ. In contrast, at depths >400 m the data fit well with the $\delta^{29}Si - [Si(OH)_4]$ trend observed for the 46.9 and 48.8°S profiles (not shown). This is in accordance with the trend in the T-S diagram (Figure 3), showing the intermediate and especially deep waters at 51°S to merge with the SAZ waters, while respective upper water column waters diverge more notably, reflecting the fact that SAMW does not reach as far south as the SAF. This zone where isotopic profiles merge corresponds to the Antarctic Intermediate Water (AAIW), which appears in the SAZ-SAF system as a salinity minimum below 500 m [*Rintoul et al.*, 2001].

[9] Southward, the latitudinal gradient toward higher Si concentrations is more pronounced. Stations at 53.7° (PFZ) and 56.9°S (IPFZ) have quite similar [$Si(OH)_4$] and also δ^{29}Si profiles in the upper 1000 m (Figure 2), but diverge between 1000 and 2500 m. In this depth zone, both profiles also diverge in their T-S plots (Figure 3). The waters below the mixed layer in the AZ-S (60.8°S) have a homogeneous δ^{29}Si signature except in bottom waters. At 63.9°S in the SIZ the 1000- to 2000-m-depth layer exhibits slightly heavier δ^{29}Si values, similar to what is observed at 56.9°S. These features remain unexplained.

[10] In general, the deep waters are isotopically homogeneous and do not show large changes of δ^{29}Si with latitude and depth. Indeed, the combined standard deviation (σ) of all the deep samples (>1800 m), is 0.06‰ (i.e., only slightly more than one σ obtained on 10 replicates, Table 1). This contrasts with the situation for silicic acid, displaying increasing concentrations with depth.

4. Discussion

4.1. Deep Water Signatures

[11] The absence of a systematic decrease of δ^{29}Si below 1800 m suggests that the progressive opal dissolution at depth is not large enough to change the dissolved Si isotopic signature there. This agrees both with model expectations [*Wischmeyer et al.*, 2003] and observations on opal dissolution with depth. Indeed, *Nelson et al.* [2002] report for the

Table 3. Seawater $\delta^{29}Si$ (Permil Versus NBS28) and $[Si(OH)_4]$ Data[a]

CTD17, 46.9°S			CTD24, 48.8°S			CTD37, 51.0°S			CTD51, 53.7°S			CTD63, 56.9°S			CTD75, 60.8°S			CTD87, 63.9°S			CTD124, 64.9°S		
Depth, m	$Si(OH)_4$, μmol L^{-1}	$\delta^{29}Si$, ‰	Depth, m	$Si(OH)_4$, μmol L^{-1}	$\delta^{29}Si$, ‰	Depth, m	$Si(OH)_4$, μmol L^{-1}	$\delta^{29}Si$, ‰	Depth, m	$Si(OH)_4$, μmol L^{-1}	$\delta^{29}Si$, ‰	Depth, m	$Si(OH)_4$, μmol L^{-1}	$\delta^{29}Si$, ‰	Depth, m	$Si(OH)_4$, μmol L^{-1}	$\delta^{29}Si$, ‰	Depth, m	$Si(OH)_4$, μmol L^{-1}	$\delta^{29}Si$, ‰	Depth, m	$Si(OH)_4$, μmol L^{-1}	$\delta^{29}Si$, ‰
5	1.8	*1.01*	4	3	*0.88*	11	5.1	*1.07*	5	10.9	1.07	5	15.7	1.01	10	27.9	1.00	6	40.8	0.97	11	61.3	0.89
25	1.9	*0.93*	50	3	*0.97*	51	5	*1.17*	30	10.9		52	15.8	0.96	31	27.7		46	46.3	0.78	41	60.5	0.78
51	1.9		99	3		101	4.9		70	11.3		100	16.2	1.00	60	27.8	0.88	101	73.6	0.77	81	60.3	0.84
76	2		150	3.2		151	5.3	*1.04*	100	11.8	1.02	141	17.3	0.95	90	28.8	1.02	151	81.1		121	60.6	0.75
101	2.6		200	3.2		201	5.8		140	13.1	1.07	174	23.1		111	45.8		202	83.3	0.67	161	63.8	
126	3.3		400	4	*0.93*	301	10.4	0.96	200	26.4		199	31.5	0.88	130	55.1	0.75	251	84.5		201	72.1	0.74
251	3.8		499	4.1	*0.82*	500	21		300	41.8		400	60.8	0.85	150	61.2		307	85.3	0.55	301	83.3	
301	3.8	*0.84*	652	7		601	25.9	0.90	401	54.8		601	73.4		200	67.7	0.62	402	87	0.54	401	90.2	
400	4.5		801	13.1	0.76	701	32.4		500	62.3	0.71	801	79	0.55	301	74.9		503	88.6		501	96.2	
500	6.8		951	22.9		799	39.5	0.66	600	68.2		1000	83.8	0.63	501	80.9	0.63	606	90.6	0.58	601	100.9	0.63
600	9.7		1103	32.6		898	45.7		699	73.5		1200	86.1		701	83.5		801	95.2	0.80	701	104.6	
700	13.6	0.77	1205	40.8	0.63	1000	54.6		800	75.7		1401	89	0.71	1000	87.4	0.65	1001	100.6	0.69	800	107.9	0.68
802	17.6		1304	48.8		1100	63.2		901	77.8		1601	93		1301	94.6		1200	106.3		901	112.6	
900	23.4		1403	54.7		1300	71.4	0.62	1000	80.3	0.66	1799	97.9	0.65	1599	102.6	0.62	1401	110.8	0.63	1000	114.1	0.60
1002	29.7	0.68	1603	70.1	0.68	1601	77.5		1200	83.1		2101	106.6	0.71	1901	110.6		1601	115.3		1101	116.7	
1101	38.3		1804	73.9		1899	82.6	0.63	1401	85.8		2400	113.6		2200	117.8	0.63	1801	122.3	0.73	1300	119.6	0.54
1200	46.3		2005	78	0.58	2200	88.8		1601	89.5		2701	121.5		2500	124.6		2000	124.2		1501	119.6	
1300	54.7		2206	81.1		2498	97.1	0.60	1801	96.1	0.54	3000	127.5	0.60	2800	130.1	0.56	2199	126		1700	116.9	
1400	60.5		2607	89.5	0.63	2800	105		2001	101		3301	133.9		3199	133.9	0.64	2501	128	0.60	1900	116.9	0.53
1500	67.3	0.65	3007	101.2	0.62	3099	115.6	0.63	2199	107	0.56	3600	140.7	0.69	3601	135.5		2801	130.1		2100	111.1	
1752	77.5		3400	117		3401	121.3	0.66	2500	115.5		3801	144.4		3899	134.5	0.67	3100	127.9	0.66	2301	102.1	
2001	81.9	0.75	3805	123.9		3704	123		2801	123.3	0.56	4001	145.4		4201	132	0.70	3400	124.3	0.60	2451	101.3	
			4166	124.4	0.50	3862	123.2	0.58	3098	127.3	0.60	4203	147.4	0.69	4352	128.2		3601	116.1		2550	100.7	0.67
															4456	119.9	0.54	3749	101.8	0.61			

[a]Station locations are identified by their CTD number and latitude. Data in italics were obtained exclusively after NH_4OH preconcentration step.

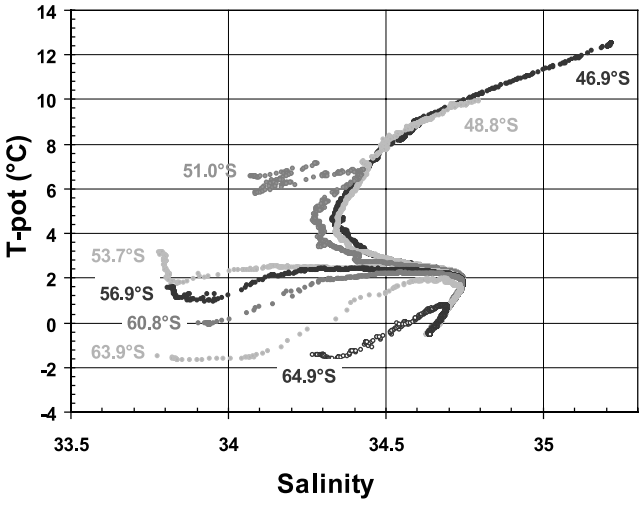

Figure 3. Potential temperature (T-pot)–salinity diagram.

Southern Ocean that most diatoms skeletons are remineralized in the upper 1000 m, and *Nelson and Gordon* [1982] observed that the Southern Ocean particulate Si remains remarkably constant between 1000 m and 3000–4000 m. The efficient remineralization of opal-dominated material fluxes in the upper 1000 m has also been pointed out by other studies [*François et al.*, 2002; *Klaas and Archer*, 2002], including in the CLIVAR-SR3 transect [*Cardinal et al.*, 2001, 2005]. At the basin scale the deep water δ^{29}Si changes are very small, falling below present methodological capabilities. As a result, the abyssal isotopic signature does not differ from model expectations for the oceanic steady state (0.70‰ [*Wischmeyer et al.*, 2003]). *De La Rocha et al.* [2000] show that the δ^{29}Si values become lighter along the deep branch of the thermohaline circulation, owing to the progressive accumulation of $Si(OH)_4$ from the dissolution of isotopically lighter biogenic silica (BSi). However, between deep Subantarctic Atlantic and deep Central Pacific waters, they report this change in δ^{29}Si to be less than 0.1‰. Therefore, considering the small area investigated in this work, we may expect an even smaller range of variation, hardly detectable by the available analytical tools.

[12] At 64.9°S, the bottom water δ^{29}Si signature (at 2550 m) is heavier by 0.14‰ compared to the signature at 1900 m. This change is also mirrored by the $Si(OH)_4$ concentrations (decreasing in bottom waters) and is likely an imprint of surface water sinking along the Antarctic slope to form Antarctic Bottom Water (AABW). It has been reported that bottom water formation occurs, among other places, off Adelie Land, close to the 64.9°S station sampled here [*Rintoul*, 1998; *Orsi et al.*, 1999; *Trull et al.*, 2001a]. The presence of AABW, clearly witnessed during the CLIVAR-SR3 cruise [see *Jacquet et al.*, 2004], therefore supplies isotopically heavy waters low in $Si(OH)_4$ to the ocean abyss.

4.2. Surface and Mesopelagic Processes

[13] Most of the Si isotopic signature variations versus latitude and depth occur in the upper 1000-m layer. In order to discuss those variations, δ^{29}Si and silicic acid contents are presented as an interpolated latitudinal transect in Figure 4. In the upper 600-m layer there is a clear trend toward heavier δ^{29}Si signatures from south to north (SIZ to SAF). The mixed layer isotopic signatures of the SAF are the heaviest observed during CLIVAR-SR-3 (δ^{29}Si = 1.12‰, Table 3). North of the SAF, in the SAZ, the trend reverses, with surface water isotopic compositions becoming lighter and similar to values observed in the PFZ and IPFZ, although SAZ waters are significantly more Si-depleted ($[Si(OH)_4] < 5$ μmol L^{-1}) compared to concentrations of 10 and 15 μmol L^{-1} for PFZ and IPFZ, respectively. In the following section we discuss possible explanations for these variations of silicon isotopes in the spring Southern Ocean.

4.2.1. Open Versus Closed Models

[14] The biologically driven Si isotopic fractionation in the mixed layer can be described in a first approximation by two simple models: (1) The Rayleigh type distillation model [*Mariotti et al.*, 1981; *De La Rocha et al.*, 1997] assumes a closed system (i.e., nutrient consumption is not replenished by external sources) and writes the evolution of the isotopic signal as

$$\delta^{29}Si_{Si(OH)4} = \delta^{29}Si_{initial} + {}^{29}\varepsilon \times \ln f. \quad (1)$$

(2) The open steady state model [e.g., *Sigman et al.*, 1999; *Varela et al.*, 2004] assumes a continuous supply of nutrients from the same external source,

$$\delta^{29}Si_{Si(OH)4} = \delta^{29}Si_{initial} - {}^{29}\varepsilon \times (1-f). \quad (2)$$

[15] In equations (1) and (2), f is defined by

$$f = \frac{[Si(OH)_4]_{observed}}{[Si(OH)_4]_{initial}}. \quad (3)$$

[16] $^{29}\varepsilon$ is the fractionation factor between opal and silicic acid (note that $^{29}\varepsilon$ is negative) and can be approximated as the difference between the δ^{29}Si signature of a single diatom and the one of the water from where it was precipitated. The $\delta^{29}Si_{initial}$ and $[Si(OH)_4]_{initial}$ are the Si isotopic composition and concentration of the silicic acid reservoir, i.e., the seawater properties before any Si consumption has taken place.

[17] Both models assume steady state conditions and a constant fractionation factor. A constant ε was supported by the experimental investigation of *De La Rocha et al.* [1997]. Indeed, these authors found it to be independent from temperature (12°–22°C range) on three tropical diatom species (for δ^{30}Si values, $^{30}\varepsilon = -1.08 \pm 0.41$‰, which corresponds to $^{29}\varepsilon = -0.56 \pm 0.21$‰, i.e., for δ^{29}Si). However, considering the relatively large uncertainty of ε deduced from experimental work, new estimates are needed, especially for the low temperature range of the Southern Ocean. On the basis of the rationale applied for δ^{15}N [e.g., *Sigman et al.*, 1999; *Altabet and François*, 2001; *Karsh et al.*, 2003], equation (1) or (2) can be used to calculate apparent ε values. Doing so and assuming

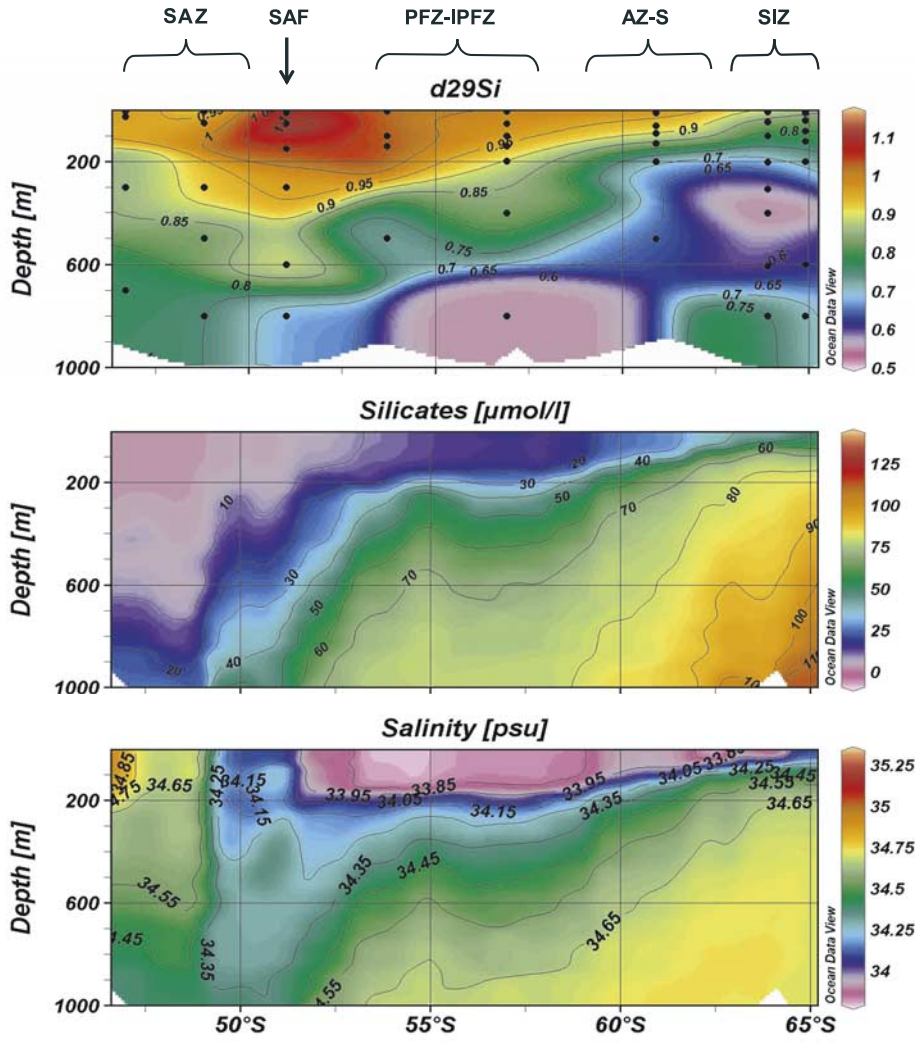

Figure 4. Interpolation of δ^{29}Si, $Si(OH)_4$ concentrations, and salinity in the upper 1000 m of the CLIVAR-SR3 latitudinal transect. Interpolation is from R. Schlitzer (Ocean Data View, 2003, available at http://www.awi-bremerhaven.de/GEO/ODV).

constant initial conditions, *Varela et al.* [2004] obtained ε estimates that were shifted toward higher absolute fractionation ($-0.88‰ < {}^{29}\varepsilon < -0.52‰$) compared to *De La Rocha et al.* [1997]. In contrast to fully controlled in vitro incubations, the in situ approach is delicate because equation (1) or (2) is unlikely to describe the system correctly. Moreover, *Wischmeyer et al.* [2003] warn against the potentially biased use of the Si isotopic signature in cases where the initial conditions of equations (1) and (2) (concentrations and isotopic signature of the source) are not constrained. Therefore the following discussion focuses first on the status of the phytoplankton activity encountered during CLIVAR-SR3, then on the identification of these initial conditions before applying a model to the data.

4.2.2. Spring Phytoplankton Activity in the Mixed Layer

[18] Before using any model describing nutrient utilization and its associated impact on Si isotopes, one must demonstrate that a significant Si-nutrient utilization has been going for some time at the moment of sampling. Previous publications have already shown that this was the case for this cruise [*Savoye et al.*, 2004a, 2004b; *Cardinal et al.*, 2005]. In Table 4 we summarize the main features of biomass and carbon fluxes during CLIVAR SR-3. Southward of the PFZ, diatoms accounted for 35 ± 15% of the total carbon biomass, while in the SAF-SAZ regions this contribution dropped to <4% [*Cardinal et al.*, 2005]. Surface BSi concentrations were up to 1.5 µmol L^{-1}, reaching between 34 and 76% of summer values for the SR-3 line section between SAZ and AZ-S, *Quéguiner* [2001] and *Beucher et al.* [2004] report for summer 1998 and 2003, respectively. During CLIVAR-SR3 new production (NP) was ~6 mmol C m^{-2} d^{-1} for the SAZ-SAF and PFZ-IPFZ systems and 16 mmol C m^{-2} d^{-1} for the SIZ-AZ-S system [*Savoye et al.*, 2004a]. These NP are somewhat lower than spring values reported for other Southern Ocean sectors [*Sambrotto and Mace*, 2000]. Nevertheless, for SAZ-SAF and PFZ-IPFZ systems, they present spring NP values that are larger than summer

Table 4. Summary of Biogeochemical Conditions Prevailing for Phytoplankton During CLIVAR-SR3 Cruise

Latitude, °S	Zone	Biomass[a] Diatoms, μgC L^{-1}	Biomass[a] Total, μgC L^{-1}	New Production,[b] mmol C m^{-2} d^{-1}	Mesopelagic C Remineralization,[c] Percent of NP	Depth, m	Spring BSi,[d] μmol kg^{-1}	Summer BSi,[e] μmol kg^{-1}
46.9	SAZ	0.3	19.5			0–50	0.10	0.75
48.8	SAZ	0.5	14.5			5	0.24	
51.0	SAF	0.2[f]	11.3[f]			5–15	0.15	0.20
...	Average SAZ-SAF	0.31 ± 0.13	15.1 ± 4.2	6.2 ± 1.8	7.5 ± 3.5		0.16	0.48
53.7	PFZ	4.2	10.9			5–90	0.38	0.9–2
56.9	IPFZ	4.6	18.2			8–90	0.86	
...	Average PFZ-IPFZ	4.4 ± 0.3	14.5 ± 5.2	5.9 ± 2.5	31 ± 0.2		0.62	1.45
60.8	AZ-S	16.2	32.3			5–100	1.52	
63.9	SIZ	10.3	20.2			0–60	0.67	1.5
64.9	SIZ	2.0	13.2			0–80	0.43	0.8
...	Average AZ-S − SIZ	9.5 ± 7	21.9 ± 9.7	16.1 ± 6	20 ± 4		0.87	1.15

See caption of Figure 1 and text for definition of acronyms.

All data are from CLIVAR SR3 spring 2001 cruise except summer BSi.

[a]Data are from phytoplankton counts at 50–60 m depth [*Cardinal et al.*, 2005].

[b]Data are from ^{15}N uptake [*Savoye et al.*, 2004a].

[c]Data are from mesopelagic (150–400 m) Ba_{xs} proxy expressed in percent from new production [*Cardinal et al.*, 2005].

[d]Data are from this study. BSi contents averaged for the given depth range. BSi was determined spectrophotometrically [*Eriksen*, 1997] after hot NaOH leaching of the particles following *Quéguiner* [2001]. The CTD were not the same as the ones from isotopic Si data and biomass but were very close.

[e]Data are from summer 1998 [*Quéguiner*, 2001] and summer 2003 [*Beucher et al.*, 2004].

[f]Biomass counts for this latitude were obtained from a CTD that has been sampled 31 days from the sampling time of the other parameters.

NP values obtained in 1998 along the northern part (SAZ-PFZ) of the same SR-3 line [*Elskens et al.*, 2002]. During CLIVAR-SR3, particle export from ^{234}Th-deficit in the mixed layer was observed at every station [*Savoye et al.*, 2004b] and mesopelagic C remineralization, estimated from the Ba_{xs} proxy, were quite significant, with the latter accounting for 20 to 31% of NP in the mixed layer at the PFZ and southward [*Cardinal et al.*, 2005]. Since there is a delay of a few weeks for the NP signal to be translated into mesopelagic C mineralization [*Cardinal et al.*, 2005], it appears that the phytoplankton activity and biomass observed during the sampling events had prevailed for 2–3 weeks prior to sampling. Such late spring activity (November) is not surprising given that significant Si-nutrient deficit has been observed even earlier (between August and September) in the SIZ, AZ-S, and PFZ [*Trull et al.*, 2001a]. Other evidence of spring activity before November is provided by SeaWiFS images showing significant Chl *a* increase from early October across most of the SR-3 line. This seasonal cycle has been discussed for earlier years (1997–1999) by *Trull et al.* [2001a, 2001b], and the year 2001–2002 showed a similar seasonality. Finally, the seasonal cycle of Si export to the deep ocean at 47°S (SAZ), 51°S (SAF), and 54°S (PFZ) shows significant BSi fluxes recorded in sediment traps well before November for the 1997–1998 season [*Trull et al.*, 2001b].

4.2.3. Assessing Initial Conditions of $Si(OH)_4$ Sources

[19] In the Southern Ocean characterized by a strong seasonality of phytoplankton growth, nutrients are supplied by vertical mixing, particularly intensive during winter and early spring, and by surface water advection from the south via Ekman drift [e.g., *Pollard et al.*, 2002; *Sarmiento et al.*, 2004]. *Sloyan and Rintoul* [2001] estimated this Ekman drift from all Southern Ocean sectors to account for 34 Sv, and its consequences for nutrient supply and biological production are discussed by *Hoppema et al.* [2003]. Given both the strong latitudinal silicic acid and Si isotopic gradients in the intermediate waters along the CLIVAR-SR3 transect (Figure 4), it is not realistic to assume a single source of silicic acid for all stations in spring. This contrasts strongly with the situation for nitrate for which relatively uniform concentrations and isotopic signatures exist for the entire deep Antarctic Zone [*Sigman et al.*, 1999]. Obviously, this is not the case for silicon, for which the observed concentration gradient results from several processes: (1) a physical control due to the shoaling of the isopycnals southward which brings nutrient-rich waters closer to the surface [*Pollard et al.*, 2002]; (2) the "silicate pump" as defined by *Dugdale et al.* [1995] consisting in a less efficient Si remineralization and dissolution in mesopelagic layers, compared to N [*Coale et al.*, 2004]; and (3) a high Si:N diatom uptake ratio in the Southern Ocean [*Brzezinski*, 1985; *Goeyens et al.*, 1998; *Brzezinski et al.*, 2003b] owing to Fe stress [e.g., *Takeda*, 1998; *Hutchins and Bruland*, 1998].

[20] These processes explain why Antarctic waters become relatively more Si-depleted from south to north, compared to nitrate [*Trull et al.*, 2001a; *Nelson et al.*, 2001; *Matsumoto et al.*, 2002; *Anderson et al.*, 2002; *Sarmiento et al.*, 2004]. The fact that we observe a significant latitudinal gradient of the isotopic signal in the mesopelagic layer but not in deep waters calls for a significant biological control. Indeed, if the isotopic gradient in intermediate waters were simply due to a water mass signature (i.e., due to the global inverse correlation between $[Si(OH)_4]$ and $\delta^{29}Si$), the $\delta^{29}Si$ versus silicic acid relationship observed for surface waters should also hold for deep waters, which is not the case. During their transport northward, the intermediate waters become progressively isotopically heavier because on a seasonal timescale they experience both mixing with surface waters and dissolution of sinking biogenic silica originating from surface waters, which themselves also display latitudinal gradient.

[21] Given the occurrence of these processes, it is unlikely that the Southern Ocean operates as a single closed system for silicon isotopes at the seasonal or annual timescale,

Table 5. Fractionation Factor Estimates (Open System), $^{29}\varepsilon$, as a Function of Spring and Winter Mixed Layer Properties[a]

		Spring Surface CLIVAR-SR3 Conditions				Winter Conditions[d]				
Zones	Lat., °S	Spring SR 3 MLD,[b] m	$[Si(OH)_4]_{ML}$ Average, μmol L^{-1}	$\delta^{29}Si_{ML}$ Average, ‰ Versus NBS28	Standard Deviation,[c] ‰	$[Si(OH)_4]_{ML}$ Winter, μmol L^{-1}	Winter MLD, m	$^{29}\varepsilon$ Shallow Winter MLD,[e] ‰	$^{29}\varepsilon$ Deep Winter MLD,[e] ‰	$^{29}\varepsilon$, ‰
SAZ	46.9	100	2.0	0.97	0.03	2.7–4.4	400–600	−0.373	−0.258	
SAZ	48.8	580	3.0	0.93	0.03	3.7–4	500–700	−0.392	−0.247	
SAF	51.0	99	5.0	1.12	0.03	3.5–5.2	170–300	NA	−0.302	
PFZ	53.7	76	11.0	1.02	NA	8–13	140–170	NA	−0.698	
IPFZ	56.9	92	15.8	0.99	0.01	8–14	140–200	−0.443	−0.217	
AZ-S	60.8	97	28.1	0.97	0.04	25–35	110–130	−0.559	−0.442	
SIZ	63.9	41	40.8	0.97	NA	40–57	75–125	−0.624	−0.644	
SIZ	64.9	104	60.7	0.84	0.03	47–63	100–200	NA	−0.632	
Average for stations south of PFZ								−0.54 ± 0.09	−0.53 ± 0.20	
Average for all stations								−0.48 ± 0.11	−0.43 ± 0.20	
All $^{29}\varepsilon$ estimates										−0.45 ± 0.17

[a]NA denotes not applicable.

[b]MLD is mixed layer depth during CLIVAR SR3 cruise (for the SAZ - PFZ: depth at which the density is 0.05 $kg.m^{-3}$ heavier than the surface density in accordance with *Rintoul and Trull* [2001a]) and for the IPFZ - SIZ depth at which the density is 0.02 $kg.m^{-3}$ heavier than the surface density in accordance with *Chaigneau et al.* [2004].

Note that the MLD at 48.8°S was exceptionally deep owing to a storm before sampling and not reflected in nutricline, so we have taken 100 m for this station.

[c]Standard deviation is calculated from the 1–4 samples analyzed in the mixed layer (ML) for each station (see Table 3).

It is NA when only one depth is analyzed in the ML for silicon isotopes.

[d]Range of winter ML conditions along SR-3 transect is as measured by *Rintoul and Bullister* [1999] in September–October 1991, *Trull et al.* [2001a] and *Rintoul and Trull* [2001] in July–August 1995 and September 1996.

[e]The ε is calculated using equations (2) and (3) (open system). Initial conditions were read on the spring CLIVAR-SR3 profiles (Table 3) at shallowest and deepest estimated winter MLD, respectively.

When no isotopic data were available from such depth, the closest deeper one has been used. It is NA when the shallow winter MLD is not applicable to the CLIVAR-SR3 situation.

See caption of Figure 1 and text for definition of acronyms.

especially in spring, during which vertical mixing can be still strong. Furthermore, *Varela et al.* [2004] report that isotopic signatures of dissolved Si and diatoms cannot be reconciled via a simple Rayleigh type model, and they report "true" ε for surface Southern Ocean waters to lie between values estimated from open and closed system models. Because the isotopic data of the CLIVAR-SR3 stations indicate strong site specificity, we will evaluate the fractionation factors defined by equation (2) for each site separately (i.e., a "multiple box approach"). This approach differs from the one discussed by *Varela et al.* [2004], who considered a single Si source along their north-south transect feeding the surface from the south. They excluded data for spring and late summer, when vertical mixing has been too intense. Since our study took place in spring only and included also the SAZ and SAF regions, we considered a different scenario; that is, each site has a unique nutrient supply from a local source located at the winter mixed layer depth (MLD). This approach is supported by the modeling results of *Wang et al.* [2001, 2003], who report that vertical nutrient supply dominates over horizontal northward advection in spring and continues to be important into summer.

[22] Winter and late winter nutrient data are available from three oceanographic cruises along the WOCE SR3 section: October 1991 [*Rintoul and Bullister*, 1999], July–August 1995, and September 1996 [*Trull et al.*, 2001a]. From Table 5 it appears that, except for the SAZ, these surface water silicate contents in winter were lower than in spring 2001. While this suggests that the conditions prevailing during CLIVAR-SR3 (November) still reflected winter, our multi-proxy data from the cruise do not support this: These data clearly show that biological activity had started at all stations as previously discussed in section 4.2.2. Therefore we favored an approach consisting in reading the initial silicate values directly from CLIVAR-SR3 profiles at a depth range likely to reflect the remnant winter surface properties, i.e., at the estimated winter MLD. In Table 5 we compare MLD range for three winter cruises covering the full SR-3 line [*Rintoul and Bullister*, 1999; *Trull et al.*, 2001a], cruises restricted to SAZ and PFZ [*Rintoul and Trull*, 2001] with the CLIVAR-SR3 spring cruise which are generally much shallower. The seasonal and interannual variations of MLD along SR-3 line have been also recently compiled and discussed by *Chaigneau et al.* [2004]. These winter MLD estimates are also in accordance with model results [*Wang and Matear*, 2001] and calculations based on satellite data [*Kara et al.*, 2003] for the same sector. They are also coherent with estimates from *Sigman et al.* [1999], who show, for the close by WOCE 19 line, that the water masses upwelling in the AZ originate from depths between the summer MLD and the Upper Circumpolar Deep Water, itself located between 250 and 500 m. Identifying the 100–200 m depth range, which includes the temperature minimum, is also consistent with *Pondaven et al.* [2000], who report unaltered remnant winter water to occur in the temperature minimum layer.

4.2.4. The ε Estimates: A MultiBox Approach

[23] As discussed above, our spring data and those of *Varela et al.* [2004] do not support the use of a closed

system Rayleigh model to describe the behavior of silicon isotopes in the Southern Ocean. Therefore we applied the open system fractionation model (equation (2)) at every station ("multiple box approach"), selecting initial conditions for silicate content and isotopic composition in order to calculate the fractionation factor, $^{29}\varepsilon$. For each station, we have determined these initial conditions from the CLIVAR-SR3 profile at the estimated winter MLD. In order to better quantify the error due to this approach (e.g., inter-annual variability), we have used a winter MLD range whenever possible, namely by calculating two $^{29}\varepsilon$ per station: for a shallow and a deep estimated winter MLD (Table 5). When no $\delta^{29}Si_{initial}$ value was available for the identified winter MLD, we took the closest deeper value.

[24] The average calculated $^{29}\varepsilon$ is -0.45 ± 0.17‰ (n = 13), which is not significantly different from the ε value obtained experimentally (-0.56 ± 0.21‰, n = 13 [*De La Rocha et al.*, 1997]). It is likely that most of the variability of our estimates comes from the uncertainties linked to equation (2) and the choice of the initial conditions. In that regard, note that the choice of mixed layer depth does not systematically bias ε estimates (e.g., deeper depths do not necessarily produce higher ε estimates as shown in Table 5), and that in general, mixing of surface and deeper waters tends to recombine waters which have experienced fractionation along the same path, and thus does not strongly influence ε estimates [*Sigman et al.*, 1999]. Although our approach is better constrained than the one based on winter nutrient data, bias could still result because our δ^{29}Si sampling resolution for intermediate waters, while high relative to previous studies, is still relatively sparse. Nevertheless, the reasonable standard deviation on ε estimated with the open system model gives confidence that the assumptions we formulated regarding spring and winter Southern Ocean characteristics are sound.

[25] Although the fractionation factor seems to be slightly larger south of the PFZ, the difference from the estimates for the SAF and SAZ is not significant (Table 5), despite quite different phytoplankton compositions and biomasses [*Savoye et al.*, 2004a; *Cardinal et al.*, 2005]. This shows that the δ^{29}Si proxy is independent of ecosystem type, validating the tool for a wide range of phytoplankton communities, temperature, and water mass conditions. A recent study on Si isotopic signatures in Lake Tanganyika further widens this conclusion to freshwater environments [*Alleman et al.*, 2004]. We recognize that our average $^{29}\varepsilon$ (-0.45‰) is smaller compared to the Southern Ocean estimates reported by *Varela et al.* [2004] ranging between -0.55 and -0.98‰. However, in their study, spring and late summer values were not taken into account and they considered one single $Si(OH)_{4initial}$ source (65 μmol L^{-1}) in the calculation of f (equation (3)) for all stations south of the PFZ. Although *Law et al.* [2003] show that vertical diffusion represents a significant pathway for Si-nutrient supply in late summer, such a single source assumption might be appropriate for summer conditions because of increased importance of Ekman transport advecting nutrient-rich surface waters from the AZ across the PF [*Sigman et al.*, 1999]. Our multiple box approach combined with the open system model neglects this northward transport which is only predominant in summer when warming and ice melting reduce vertical mixing [*Trull et al.*, 2001a; *Wang et al.*, 2001, 2003]. Our Si isotopes results support this view for spring in the Southern Ocean as long as the initial Si conditions can be identified. In this regard, note that the application of the closed Rayleigh type model to each of our stations gave very low fractionation factor estimates (-0.32 ± 0.11). Similarly, considering one system with a single southern Si-source [*Varela et al.*, 2004] yields to a fractionation factor of -0.32 ± 0.13 (open system) and -0.20 ± 0.16 (closed system). Removing the SAZ stations from such single system calculation does improve the standard deviation, but the fractionation factor obtained is even lower. We are in the process of assessing Si isotopic signatures of diatoms sampled during CLIVAR-SR3 in order to better constrain and compare these estimates with those of *Varela et al.* [2004], who derived from their measurements an estimate of $^{29}\varepsilon$ between diatoms and seawater of -0.80‰. Other siliceous organisms might also be studied more systematically. For instance, at the PFZ-IPFZ CLIVAR-SR3 stations, silicoflagellates accounted for a significant part of the biomass [*Cardinal et al.*, 2005]. Since little is known about their contribution to the silicon cycle, their impact on the overall Si-isotopic signature cannot be evaluated. Clearly, as stressed by the few studies on silicon isotopes, there is a serious need for a more substantial data set in the modern ocean in order to better understand the processes controlling Si isotopic fractionation.

4.2.5. Surface Latitudinal Variations and Nutrient Utilization

[26] The isotopic compositions of surface waters in the SAZ are less heavy than predicted by the model of *Wischmeyer et al.* [2003] from the extent of silicate depletion. For instance, the 46.9°S surface δ^{29}Si is +0.97‰ with $[Si(OH)_4]$ less than 2 μmol L^{-1}. This isotopic signature is very similar to the one observed at 60.8°S (AZ-S), but the silicate concentration there reaches 28 μmol L^{-1}. This discrepancy with the model might be partly ascribed to a seasonal effect. Indeed, our study took place in late spring, whereas the surface water isotopic compositions modeled by *Wischmeyer et al.* [2003] reflect annual averages. It is likely that our surface water isotopic signatures would progressively shift toward heavier values with progress of the season [*Wischmeyer et al.*, 2003; *Varela et al.*, 2004].

[27] Another explanation can be drawn from Figure 5, where we compare the relative Si utilization ($[1 - f]$) calculated from mixed layer silicate and the initial concentration as defined in Table 5 (average silicate over the winter MLD range) with our spring mixed layer isotopic signatures. While both parameters correlate for stations south of the PFZ ($r^2 = 0.84$), the SAZ-SAF stations do not fit the regression, especially for the SAZ. Assuming a constant $\delta^{29}Si_{initial}$ at all stations the slope of such regression line is an estimate of $^{29}\varepsilon$ [*Varela et al.*, 2004]. For the five southernmost stations, we obtain a $^{29}\varepsilon$ of -0.54 ± 0.14 (significant at $p < 0.03$), which is within the range of our estimates calculated from all stations in Table 5. This reflects that the variations of $[Si(OH)_4]_{initial}$ between southernmost stations (taken into account in Figure 5 through the

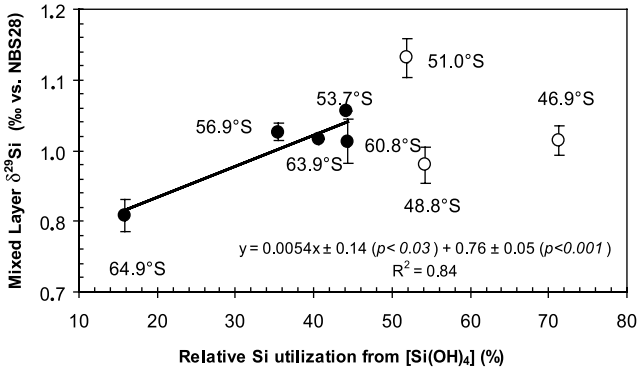

Figure 5. Mixed layer average $\delta^{29}Si$ versus relative Si utilization. Relative Si utilization ($1 - f$) was calculated by equation (3). $[Si(OH)_4]_{initial}$ was the average concentration from Table 3 at a depth range estimated for the winter MLD (Table 5). Error bars on $\delta^{29}Si$ are the standard deviation obtained on the average $\delta^{29}Si$ calculated on all samples analyzed in the mixed layer (between one and four for each station).

calculation of f) has larger influence than the $\delta^{29}Si_{initial}$ on the calculation of $^{29}\varepsilon$. In contrast, the changes in both $[Si(OH)_4]_{initial}$ and $\delta^{29}Si_{initial}$ must be considered in the SAZ-SAF system to obtain $^{29}\varepsilon$ estimates that are not significantly different from the other southern stations (Table 5). Therefore, Figure 5 emphasizes again that mixed layer isotopic signature is not a simple reflection of the Si concentration but that latitudinal differences in physical and biogeochemical processes in the mesopelagic zone affect the surface isotopic signature, chiefly in setting initial conditions before growth onset.

4.3. Paleoceanographic Implications

[28] As also stated by *Wischmeyer et al.* [2003], time and spatial variations of initial conditions must be better constrained to interpret the $\delta^{29}Si$ as a proxy of relative Si utilization in the past, especially because the interpretation of sedimentary diatom-associated Si-isotopic signals is of great relevance in paleoceanography [cf. *Anderson et al.*, 2002; *Crosta and Shemesh*, 2002; *Brzezinski et al.*, 2002; *Robinson et al.*, 2004]. The debate is still open as to whether or not Southern Ocean fronts were shifted northward in the Last Glacial Maximum compared to the Holocene [e.g., *Wells and Connell*, 1997; *Asmus et al.*, 1999; *Moore et al.*, 2000; *Dezileau et al.*, 2003], and sea ice extent and vertical mixing are also parameters that could have changed through time with a probable glacial enhanced water stratification [*François et al.*, 1997; *Sigman et al.*, 2004]. All these processes have shaped the nutrient characteristics of the Southern Ocean water masses and surface silicate pump. Therefore Quaternary sedimentary records integrate variations of surface phytoplankton activity with potential latitudinal shifts of the properties (concentration and isotopic signature) of the waters upwelling in the Antarctic Circumpolar Current. Our detailed modern $\delta^{29}Si$ data set highlights large isotopic variations in the surface and intermediate Southern Ocean waters even within a single functional zone. For paleoceanographic reconstructions this makes it difficult to decipher between changes in relative utilization and initial conditions. Our present range of estimates for $\delta^{29}Si_{initial}$ (0.25‰, from 0.71 in the PFZ to 0.96‰ in the SAF) is significant in regard to the 0.3–0.4‰ changes observed between LGM and Holocene Southern Ocean diatoms [*De La Rocha et al.*, 1998]. Therefore, although this does not contradict the qualitative conclusions drawn to date from sedimentary $\delta^{30}Si$ records [*De La Rocha et al.*, 1998; *Brzezinski et al.*, 2002], highlighting a relatively reduced Si utilization south of the PFZ during glacials, it is likely that these records actually integrate information from a larger area than just the overlying water column.

5. Conclusions

[29] By doubling the open ocean Si isotopes database, this study presents significant insights on this new proxy that carries a high potential for paleoceanographic studies. The large depth and latitudinal $\delta^{29}Si$ coverage achieved, which includes the different functional zones of the Southern Ocean from Subantarctic to ice edge, highlights significant variability. Such variability does not corroborate the concept that Southern Ocean surface waters operate as a closed system during spring. The deep waters are found to be isotopically homogenous, whereas in the mesopelagic waters a north-south gradient toward lighter signature is observed. In the mixed layer, this latitudinal trend is more pronounced, except in the SAZ whose isotopic signatures are not heavier than in the PFZ-IPFZ system, although these northern stations are much more Si-depleted.

[30] To examine the origins of the observed isotopic variations, we applied a multiple box approach based on the open system concept [*Sigman et al.*, 1999] to assess the Si fractionation between seawater and diatoms associated with uptake. We did not observe significant latitudinal differences, and our average result ($^{29}\varepsilon = -0.45 \pm 0.17$‰) is similar to the one reported by *De La Rocha et al.* [1997]. This gives support to the use of the $\delta^{29}Si$ proxy for a wide range of ecosystems and environments, including freshwater systems [*Alleman et al.*, 2004]. Nevertheless, this study underlines the necessity to further monitor variations of the Si isotopic signatures in the modern ocean in order to better validate this proxy for past reconstructions. In particular, constraining the dissolved Si isotopic fingerprint of waters below the mixed layer is essential to investigate the processes which dominate nutrient resupply to the mixed layer. The development of such a data set would also open other applications of silicon isotopes in the context of the current global silicon cycle (water masses and circulation) and ocean nutrient limitation (e.g., Si versus Fe limitation).

[31] **Acknowledgments.** We would like to thank the CLIVAR SR3 party onboard the R/V *Aurora Australis*, especially the officers and crew and S. Rintoul (chief scientist) for their efficient support. We thank C. Curran and S. Bray (ACE-CRC) for nutrient analyses and C. Beucher (U. Brest) for advice on the chemical processing of seawater samples prior to isotopic analyses. We are grateful to J. de Jong and N. Mattielli (ULB) for the management of the MC-ICP-MS lab in Brussels, to L. Monin and N. Dahkani (MRAC) for their efficient help in sample processing and ICP-AES analyses, and to D. van Aubel (MRAC) for artwork. M. Elskens (VUB) is acknowl-

edged for his useful assistance in low-level silicic acid colorimetric analyses. This manuscript has greatly benefited from the constructive reviews of M. Brzezinski and D. Wolf-Gladrow. This work was conducted under the BELCANTO II network funded by the Belgian Science Policy on Sustainable Development (SPSDII, contracts EV/37/7C and EV/03/7A). Fieldwork was supported by the Australian Antarctic Science program via projects ASAC 1156 (T. W. T.) and 1343 (F. D.).

References

Alleman, L. Y., D. Cardinal, C. Cocquyt, P.-D. Plisnier, and L. André (2004), Si isotopes to constrain the biogenic Si utilisation in Lake Tanganyika, *Geophys. Res. Abstr.*, *6*, 05175.

Altabet, M. A., and R. François (2001), Nitrogen isotope biogeochemistry of the Antarctic Polar Frontal Zone at 170°W, *Deep Sea Res., Part II*, *48*, 4247–4273.

Anderson, R. F., Z. Chase, M. Q. Fleisher, and J. Sachs (2002), The Southern Ocean's biological pump during the Last Glacial Maximum, *Deep Sea Res., Part II*, *49*, 1909–1938.

Asmus, T., M. Frank, C. Koschmieder, N. Frank, R. Gersonde, G. Kuhn, and A. Mangini (1999), Variations of biogenic particle flux in the southern Atlantic section of the Subantarctic Zone during the late Quaternary: Evidence from sedimentary $^{231}Pa_{ex}$ and $^{230}Th_{ex}$, *Mar. Geol.*, *159*, 63–78.

Beucher, C., P. Tréguer, A.-M. Hapette, R. Corvaisier, N. Metzl, and J.-J. Pichon (2004), Intense summer Si-recycling in the surface Southern Ocean, *Geophys. Res. Lett.*, *31*, L09305, doi:10.1029/2003GL018998.

Brzezinski, M. A. (1985), The Si: C: N ratio of marine diatoms: Interspecific variability and the effect of some environmental variables, *J. Phycol.*, *21*, 347–357.

Brzezinski, M. A., C. J. Pride, V. M. Franck, D. M. Sigman, J. L. Sarmiento, K. Matsumoto, N. Gruber, G. H. Rau, and K. H. Coale (2002), A switch from $Si(OH)_4$ to NO_3^- depletion in the glacial Southern Ocean, *Geophys. Res. Lett.*, *29*(12), 1564, doi:10.1029/2001GL014349.

Brzezinski, M. A., J. L. Jones, K. D. Bidle, and F. Azam (2003a), The balance between silica production and silica dissolution in the sea: Insights from Monterey Bay, California, applied to the global data set, *Limnol. Oceanogr.*, *48*, 1846–1854.

Brzezinski, M. A., M.-L. Dickson, D. M. Nelson, and R. Sambrotto (2003b), Ratios of Si, C and N uptake by microplankton in the Southern Ocean, *Deep Sea Res., Part II*, *50*, 619–633.

Cardinal, D., F. Dehairs, T. Cattaldo, and L. André (2001), Geochemistry of suspended particles in the Subantarctic and Polar Front Zones south of Australia: Constraints on export and advection processes, *J. Geophys. Res.*, *106*(C12), 31,637–31,656.

Cardinal, D., L. Y. Alleman, J. De Jong, K. Ziegler, and L. André (2003), Isotopic composition of silicon measured by multicollector plasma source mass spectrometry in dry plasma mode, *J. Anal. At. Spectrom.*, *18*, 213–218, doi:10.1039/b210109b.

Cardinal, D., N. Savoye, T. W. Trull, L. André, E. E. Kopczynska, and F. Dehairs (2005), Variations of carbon remineralisation in the Southern Ocean illustrated by the Ba_{xs} proxy, *Deep Sea Res., Part I*, *52*, 355–370, doi:10.106/j.dsr.2004.10.002.

Carignan, J., D. Cardinal, A. Eisenhauer, A. Galy, M. Rehkämper, F. Wombacher, and N. Vigier (2004), A reflection on Mg, Cd, Ca, Li and Si isotopic measurements and related reference materials, *Geostand. Geoanal. Res.*, *28*, 139–148.

Chaigneau, A., R. A. Morrow, and S. R. Rintoul (2004), Seasonal and interannual evolution of the mixed layer in the Antarctic Zone south of Tasmania, *Deep Sea Res., Part I*, *51*, 2047–2072.

Coale, K. H., et al. (2004), Southern Ocean iron enrichment experiment: carbon cycling in high- and low-Si waters, *Science*, *304*, 408–414.

Crosta, X., and A. Shemesh (2002), Reconciling down core anticorrelation of diatom carbon and nitrogen isotopic ratios from the Southern Ocean, *Paleoceanography*, *17*(1), 1010, doi:10.1029/2000PA000565.

de Freitas, A. S. W., A. W. McCulloch, and A. G. McInnes (1991), Recovery of silica from aqueous silicate solutions via trialkyl or tetraalkylammonium silicomolybdate, *Can. J. Chem.*, *69*, 611–614.

De La Rocha, C. L. (2002), Measurement of silicon stable isotope natural abundances via multicollector inductively coupled plasma mass spectrometry (MC-ICP-MS), *Geochem. Geophys. Geosyst.*, *3*(8), 1045, doi:10.1029/2002GC000310.

De La Rocha, C. L., M. A. Brzezinski, and M. J. DeNiro (1996), Purification, recovery and laser-driven fluorination of silicon from dissolved and particulate silica for the measurement of natural stable isotope abundances, *Anal. Chem.*, *68*, 3746–3750.

De La Rocha, C. L., M. A. Brzezinski, and M. J. DeNiro (1997), Fractionation of silicon isotopes by marine diatoms during biogenic silica formation, *Geochim. Cosmochim. Acta*, *61*, 5051–5056.

De La Rocha, C. L., M. A. Brzezinski, M. J. DeNiro, and A. Shemesh (1998), Silicon-isotope composition of diatoms as an indicator of past oceanic change, *Nature*, *395*, 680–683.

De La Rocha, C. L., M. A. Brzezinski, and M. J. DeNiro (2000), A first look at the distribution of the stable isotopes of silicon in natural waters, *Geochim. Cosmochim. Acta*, *64*, 2467–2477.

Dezileau, L., J. L. Reyss, and F. Lemoine (2003), Late Quaternary changes in biogenic opal fluxes in the Southern Indian Ocean, *Mar. Geol.*, *202*, 143–158.

Dugdale, R. C., F. P. Wilkerson, and H. J. Minas (1995), The role of a silicate pump in driving new production, *Deep Sea Res., Part I*, *42*, 697–719.

Elskens, M., F. Dehairs, B. Griffiths, and T. Cattaldo (2002), N uptake conditions during summer in the Subantarctic and Polar Front Zones of the Australian sector of the Southern Ocean, *J. Geophys. Res.*, *107*(C11), 3182, doi:10.1029/2001JC000897.

Eriksen, R. (1997), A practical manual for the determination of salinity, dissolved oxygen, and nutrients in seawater, *Res. Rep. 11*, 83 pp., Antarct. Coop. Res. Cent., Hobart, Tasmania, Australia.

François, R., M. A. Altabet, E.-F. Yu, D. Sigman, M. P. Bacon, M. Frank, G. Bohrmann, G. Bareille, and L. D. Labeyrie (1997), Contribution of Southern Ocean surface-water stratification to low atmospheric CO_2 concentrations during the last glacial period, *Nature*, *389*, 929–935.

François, R., S. Honjo, R. Krishfield, and S. Manganini (2002), Factors controlling the flux of organic carbon to the bathypelagic zone of the ocean, *Global Biogeochem. Cycles*, *16*(4), 1087, doi:10.1029/2001GB001722.

Goeyens, L., M. Semeneh, M. E. M. Baumann, M. Elskens, D. Shopova, and F. Dehairs (1998), Phytoplankton nutrient utilisation and nutrient signature in the Southern Ocean, *J. Mar. Syst.*, *17*, 143–157.

Henderson, G. M. (2002), New oceanic proxies for paleoclimate, *Earth Planet. Sci. Lett.*, *203*, 1–13.

Hoppema, M., H. J. W. de Baar, E. Fahrbach, H. H. Hellmer, and B. Klein (2003), Substantial advective iron loss diminishes phytoplankton production in the Antarctic Zone, *Global Biogeochem. Cycles*, *17*(1), 1025, doi:10.1029/2002GB001957.

Hutchins, D. A., and K. W. Bruland (1998), Iron-limited diatom growth and Si:N uptake ratios in a coastal upwelling regime, *Nature*, *393*, 561–564.

Jacquet, S. H. M., F. Dehairs, and S. Rintoul (2004), A high resolution transect of dissolved barium in the Southern Ocean, *Geophys. Res. Lett.*, *31*, L14301, doi:10.1029/2004GL020016.

Kara, A. B., P. A. Rochford, and H. E. Hurlburt (2003), Mixed layer depth variability over the global ocean, *J. Geophys. Res.*, *108*(C3), 3079, doi:10.1029/2000JC000736.

Karl, D. M., and G. Tien (1992), MAGIC: A sensitive and precise method for measuring dissolved phosphorus in aquatic environments, *Limnol. Oceanogr.*, *37*, 105–116.

Karsh, K. L., T. W. Trull, M. J. Lourey, and D. M. Sigman (2003), Relationship of nitrogen isotope fractionation to phytoplankton size and iron availability during the Southern Ocean Iron RElease Experiment (SOIREE), *Limnol. Oceanogr.*, *48*, 1058–1068.

Klaas, C., and D. E. Archer (2002), Association of sinking organic matter with various types of mineral ballast in the deep sea: Implications for the rain ratio, *Global Biogeochem. Cycles*, *16*(4), 1116, doi:10.1029/2001GB001765.

Law, C. S., E. R. Abraham, A. J. Watson, and M. I. Liddicoat (2003), Vertical eddy diffusion and nutrient supply to the surface mixed layer of the Antarctic Circumpolar Current, *J. Geophys. Res.*, *108*(C8), 3272, doi:10.1029/2002JC001604.

Mariotti, A., J. C. Germon, P. Hubert, P. Kaiser, R. Letolle, A. Tardieux, and P. Tardieux (1981), Experimental determination of nitrogen kinetic isotope fractionation: Some principles—Illustration for the denitrification and nitrification processes, *Plant Soil*, *62*, 413–430.

Martin, J. H. (1990), Glacial-interglacial change: The iron hypothesis, *Paleoceanography*, *5*(1), 1–13.

Matsumoto, K., J. L. Sarmiento, and M. A. Brzezinski (2002), Silicic acid leakage from the Southern Ocean: A possible explanation for glacial atmospheric pCO_2, *Global Biogeochem. Cycles*, *16*(3), 1031, doi:10.1029/2001GB001442.

Metzl, N., B. Tilbrook, and A. Poisson (1999), The annual fCO_2 cycle in the sub-Antarctic Ocean, *Tellus, Ser. B*, *51*, 849–861.

Milligan, A. J., D. E. Varela, M. A. Brzezinski, and F. M. M. Morel (2004), Dynamics of silicon metabolism and silicon isotopic discrimination in a marine diatom as a function of pCO_2, *Limnol. Oceanogr.*, *49*, 322–329.

Moore, J. K., M. R. Abbott, J. R. Richman, and D. M. Nelson (2000), The Southern Ocean at the Last Glacial Maximum: A strong sink for atmospheric carbon dioxide, *Global Biogeochem. Cycles*, *14*(1), 455–475.

Nelson, D. M., and L. I. Gordon (1982), Production and pelagic dissolution of biogenic silica in the Southern Ocean, *Geochim. Cosmochim. Acta*, *46*, 491–501.

Nelson, D. M., M. A. Brzezinski, D. E. Sigmon, and V. M. Franck (2001), A seasonal progression of Si limitation in the Pacific sector of the Southern Ocean, *Deep Sea Res., Part II*, *48*, 3973–3995.

Nelson, D. M., et al. (2002), Vertical budgets for organic carbon and biogenic silica in the Pacific sector of the Southern Ocean, 1996–1998, *Deep Sea Res., Part II*, *49*, 1645–1674.

Orsi, A., T. Whitworth III, and W. D. Nowlin (1995), On the meridional extent and fronts of the Antarctic Circumpolar Current, *Deep Sea Res., Part I*, *42*, 641–673.

Orsi, A. H., G. C. Johnson, and J. L. Bullister (1999), Circulation, mixing, and production of Antarctic Bottom Water, *Prog. Oceanogr.*, *43*, 55–109.

Pollard, R. T., M. I. Lucas, and J. F. Read (2002), Physical controls on biogeochemical zonation in the Southern Ocean, *Deep Sea Res., Part II*, *49*, 3289–3305.

Pondaven, P., O. Ragueneau, P. Tréguer, A. Hauverspre, L. Dezileau, and J.-L. Reyss (2000), Resolving the 'opal paradox' in the Southern Ocean, *Nature*, *405*, 168–172.

Popova, E. E., V. A. Ryabchenko, and M. J. R. Fasham (2000), Biological pump and vertical mixing in the Southern Ocean: Their impact on atmospheric CO_2, *Global Biogeochem. Cycles*, *14*(1), 477–798.

Quéguiner, B. (2001), Biogenic silica production in the Australian sector of the Subantarctic Zone of the Southern Ocean in late summer 1998, *J. Geophys. Res.*, *106*, 31,627–31,636.

Rintoul, S. R. (1998), On the origin and influence of Adelie Land Bottom Water, in *Ocean, Ice and Atmosphere: Interactions at the Antarctic Continental Margin*, *Antarct. Res. Ser.*, vol. 75, edited by S. S. Jacobs and R. F. Weiss, pp. 151–171, AGU, Washington, D. C.

Rintoul, S. R., and J. L. Bullister (1999), A late winter hydrographic section from Tasmania to Antarctica, *Deep Sea Res., Part I*, *46*, 1417–1454.

Rintoul, S. R., and T. W. Trull (2001), Seasonal evolution of the mixed layer in the Subantarctic Zone south of Australia, *J. Geophys. Res.*, *106*(C12), 31,447–31,462.

Rintoul, S. R., C. W. Hughes, and D. Olbers (2001), The Antarctic Circumpolar Current System, in *Ocean Circulation and Climate*, *Int. Geophys. Ser.*, vol. 77, edited by G. Siedler, J. Church, and J. Gould, pp. 271–302, Elsevier, New York.

Robinson, R. S., B. G. Brunelle, and D. M. Sigman (2004), Revisiting nutrient utilization in the glacial Antarctic: Evidence from a new method for diatom-bound N isotopic analysis, *Paleoceanography*, *19*, PA3001, doi:10.1029/2003PA000996.

Sambrotto, R. N., and B. J. Mace (2000), Coupling of biological and physical regimes across the Antarctic Polar Front as reflected by nitrogen production and recycling, *Deep Sea Res., Part II*, *47*, 3339–3367.

Sarmiento, J. L., N. Gruber, M. A. Brzezinski, and J. P. Dunne (2004), High-latitude controls of thermocline nutrients and low latitude biological productivity, *Nature*, *427*, 56–60.

Savoye, N., F. Dehairs, M. Elskens, D. Cardinal, E. E. Kopczyñska, T. W. Trull, S. Wright, W. Baeyens, and F. B. Griffiths (2004a), Regional variation of spring N-uptake and new production in the Southern Ocean, *Geophys. Res. Lett.*, *31*, L03301, doi:10.1029/2003GL018946.

Savoye, N., K. O. Buesseler, D. Cardinal, and F. Dehairs (2004b), ^{234}Th deficit and excess in the Southern Ocean during spring 2001: Particle export and mineralization, *Geophys. Res. Lett.*, *31*, L12301, doi:10.1029/2004GL019744.

Sigman, D. M., M. A. Altabet, D. C. McCorkle, R. François, and G. Fischer (1999), The δ^{15}N of nitrate in the Southern Ocean: Consumption of nitrate in surface waters, *Global Biogeochem. Cycles*, *13*(4), 1149–1166.

Sigman, D. M., S. L. Jaccard, and G. H. Haug (2004), Polar ocean stratification in a cold climate, *Nature*, *428*, 59–63.

Sloyan, B. M., and S. R. Rintoul (2001), The Southern Ocean limb of the global deep overturning circulation, *J. Phys. Oceanogr.*, *31*, 143–173.

Strickland, J. D. H., and T. R. Parsons (1968), *A Practical Handbook of Seawater Analysis*, Fish. Res. Board of Can., 311 pp., Ottawa.

Takahashi, T., et al. (2002), Global sea–air CO_2 flux based on climatological surface ocean pCO_2, and seasonal biological and temperature effects, *Deep Sea Res., Part II*, *49*, 1601–1622.

Takeda, S. (1998), Influence of iron availability on nutrient consumption ratio of diatoms in oceanic waters, *Nature*, *393*, 774–777.

Trull, T., S. R. Rintoul, M. Hadfield, and E. R. Abraham (2001a), Circulation and seasonal evolution of polar waters south of Australia: Implications for iron fertilization of the Southern Ocean, *Deep Sea Res., Part II*, *48*, 2439–2466.

Trull, T., S. Bray, S. Manganini, S. Honjo, and R. François (2001b), Moored sediment trap measurements of carbon export in the Sub-Antarctic and Polar Front Zones of the Southern Ocean, south of Australia, *J. Geophys. Res.*, *106*, 31,489–31,510.

Varela, D., C. J. Pride, and M. A. Brzezinski (2004), Biological fractionation of silicon isotopes in Southern Ocean surface waters, *Global Biogeochem. Cycles*, *18*, GB1047, doi:10.1029/2003GB002140.

Wang, W., and R. J. Matear (2001), Modeling the upper ocean dynamics in the Subantarctic and Polar Frontal Zones in the Australian sector of the Southern Ocean, *J. Geophys. Res.*, *106*(C12), 31,511–31,524.

Wang, X., R. J. Matear, and T. W. Trull (2001), Modeling seasonal phosphate export and resupply in the Subantarctic and Polar Frontal Zones in the Australian sector of the Southern Ocean, *J. Geophys. Res.*, *106*(C12), 31,525–31,542.

Wang, X., R. J. Matear, and T. W. Trull (2003), Nutrient utilization ratios in the Polar Frontal Zone in the Australian sector of the Southern Ocean: a model, *Global Biogeochem. Cycles*, *17*(1), 1009, doi:10.1029/2002GB001938.

Watson, A. J., D. C. E. Bakker, A. J. Ridgwell, P. W. Boyd, and C. S. Law (2000), Effect of iron supply on Southern Ocean CO_2 uptake and implications for glacial atmospheric CO_2, *Nature*, *407*, 730–733.

Wells, P. E., and R. Connell (1997), Movement of hydrological fronts and widespread erosional events in the southwestern Tasman Sea during the Late Quaternary, *Aust. J. Earth Sci.*, *44*, 105–112.

Wischmeyer, A. G., C. L. De La Rocha, E. Maier-Reimer, and D. A. Wolf-Gladrow (2003), Control mechanisms for the oceanic distribution of silicon isotopes, *Global Biogeochem. Cycles*, *17*(3), 1083, doi:10.1029/2002GB002022.

Wombacher, F., and M. Rehkämper (2004), Problems and suggestions concerning the notation of cadmium stable isotope compositions and the use of reference materials, *Geostand. Geoanal. Res.*, *28*, 173–178.

Yool, A., and T. Tyrrell (2003), Role of diatoms in regulating the ocean's silicon cycle, *Global Biogeochem. Cycles*, *17*(4), 1103, doi:10.1029/2002GB002018.

L. Y. Alleman, Ecole Supérieure des Mines de Douai, Douai, France.

L. André and D. Cardinal, Department of Geology and Mineralogy, Musée Royal de l'Afrique Centrale, Leuvensesteenweg 13, B-3080 Tervuren, Belgium. (damien.cardinal@africamuseum.be)

F. Dehairs and N. Savoye, Department of Analytical and Environmental Chemistry, Vrije Universiteit Brussel, Pleinlaan 2, B-1050 Brussels, Belgium. (fdehairs@vub.ac.be)

T. W. Trull, Antarctic Climate and Ecosystem Cooperative Research Centre, CSIRO Marine Research, University of Tasmania, Private Bag 80, Hobart, 7001 Tasmania, Australia. (tom.trull@utas.edu.au)